THE JOURNAL OF PHYSICAL CHEMISTRY B

Article

pubs.acs.org/JPCB

Fluorescence Quenching Studies of γ-Butyrolactone Binding Protein (CprB) from *Streptomyces coelicolor* A3(2)

Anwesha Biswas,[†] Ravi K. Swarnkar,[†] Bhukya Hussain,[†,‡] Suraj K. Sahoo,[†] P. I. Pradeepkumar,[†] G. Naresh Patwari,*[,†] and Ruchi Anand*[,†]

[†]Department of Chemistry, Indian Institute of Technology Bombay, Mumbai, Maharashtra 400076, India

Supporting Information

ABSTRACT: Quorum sensing is a cell density dependent phenomenon that utilizes small molecule inducers like γ-butyrolactones (GBLs) and their receptor proteins for adaptation to the environment. The cognate GBLs that bind to several of this GBL receptor family of proteins remain elusive. Here, using CprB protein from *Streptomyces coelicolor* A3(2) as a model system, we devise a method suited for ligand screening that would be applicable to the entire family of GBL receptors. Docking studies were performed to confirm the identity of the ligand binding pocket, and it was ascertained that the common γ-butyrolactone moiety interacts with the conserved tryptophan residue (W127) residing in the ligand binding pocket. The presence of W127 in the cavity was exploited to monitor its fluorescence quenching on the addition of two chemically synthesized GBLs. Analysis of the data with both the native and W185L mutant versions of the protein confirmed that the compounds used as quenchers reside in the ligand binding pocket. Furthermore, fluorescence lifetime and potassium iodide (KI) quenching studies established that the quenching is static in nature and that the tryptophan residue is buried and inaccessible to surface quenchers. Additionally, a combination of concentration dependent fluorescence quenching and dynamic light scattering experiments revealed that the binding properties of the protein are concentration dependent and it was concluded that the most efficient binding of the ligand is evoked by working at the lowest concentration of protein, providing a sufficient signal, where the aggregation effects are negligible.

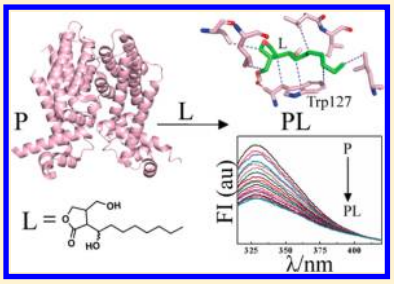

INTRODUCTION

Bacteria employ a response mechanism termed quorum sensing to regulate certain transcription and gene expression processes that in several instances lead to activation of secondary metabolic pathways.[1−3] Quorum sensing involves small signaling molecules called autoinducers, exuded by the bacteria, which trigger a response at a threshold concentration by binding to their receptor proteins.[4] The response is therefore cell density dependent and is elicited as a consequence of the protein−autoinducer complex formation. Extensive work on such systems has unearthed numerous classes of these signaling molecules like the *N*-acylhomoserine lactones (AHLs),[3,5,6] 4-hydroxy-2-alkyl quinolines (HAQs),[7,8] γ-butyrolactones (GBLs),[9,10] cyclic and linear oligopeptides,[11,12] etc. A GBL from *Streptomyces griseus* named A-factor (2-isocaprylolyl-3R-hydroxymethyl-butyrolactone) was first among the butanolides that have been identified.[13] It was established in 1994 by Horinouchi and co-workers that A-factor effectively triggers morphological differentiation and streptomycin production in this species by binding to its receptor protein ArpA.[14−17] Subsequently, other GBLs and the transcription factors they regulate have been identified in several species of *Streptomyces*.[18−21]

There is, however, a paucity of X-ray structural information available in the GBL receptor family of proteins. CprB from *S. coelicolor* A3(2),[22] predicted to be a homologue of ArpA, is the only member for which the structure has been elucidated in the apo form (Figure 1).[23,24] The structure confirmed the presence of two domains: an N-terminal DNA binding domain, similar to the tetracycline receptor family of antibiotic resistance proteins,[25] and a divergent C-terminal ligand binding domain (the regulatory domain) that is proposed to bind the cognate quorum sensing molecule. The protein exists in a dimeric state with the two units being related by a pseudo-2-fold axis.[24] The regulatory domain which is of the most interest for our study is composed of an antiparallel bundle of five helices (α5−α10) with helix α6 forming the base of the cavity. The large cavity thus created that has a depth of approximately 20 Å and a diameter of 5 Å is lined by hydrophobic residues.

Comparison of GBL binding proteins showed that most of the residues in the pocket although hydrophobic in nature are not strictly conserved. Interestingly, the pocket contains a tryptophan residue at the 127 position (Figure 1) which is conserved among all the members of this family.[15] Mutation of the corresponding tryptophan residue W119 in ArpA (W127 for CprB) abolished the A-factor binding properties of the protein completely, thereby signifying its importance in GBL binding.[15] This also indicated that, apart from the few conserved residues within the pocket, the rest have been fine-tuned in each member of the family of proteins to recognize

Received: April 12, 2014
Revised: July 9, 2014
Published: July 30, 2014

dx.doi.org/10.1021/jp503589h | J. Phys. Chem. B 2014, 118, 10035−10042

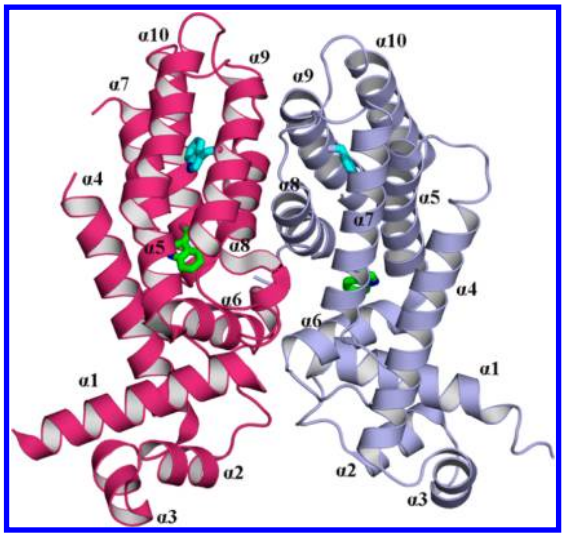

Figure 1. Structure of the dimeric protein CprB (PDB ID: 1UI5) with the monomeric units represented in pink and light blue; rings of W127 and W185 are shown in green and cyan, respectively.

their specific butanolides.[24] Additionally, CprB contains a second tryptophan residue at position 185 in the sequence, which is less conserved and not a part of the pocket described earlier.

The primary motive of this work was to confirm the entry of the ligand in the pocket of the regulatory domain and also monitor the ligand binding ability of the protein CprB. Since CprB was essentially identified as a GBL receptor, our ligand binding studies were performed with two chemically synthesized GBLs. Changes in the fluorescence emission characteristics of the conserved tryptophan (W127) were employed to assess the ligand binding in both the native and W185L mutant (single tryptophan system) forms of the protein. Furthermore, to confirm whether quenching is static or dynamic in nature and to gauge the surface accessibility of the tryptophan residues, fluorescence lifetime and potassium iodide (KI) quenching studies were performed, respectively. Additionally, using a combination of concentration dependent fluorescence quenching and dynamic light scattering experiments, the aggregation state of the protein was also probed.

EXPERIMENTAL METHODS

Docking Studies. The most probable active site in a protein for a ligand molecule can be determined using the blind docking method. The same approach was used for the present study to identify the ligand binding pocket in the protein as well as screen a set of nine different ligands. The 2.4 Å X-ray structure of CprB (PDB ID: 1UI5) was downloaded from the RCSB protein data bank, and its monomeric unit was used for docking calculations. 250 docking runs were conducted by using AutoDock version 4.2,[26] and the Darwinian *genetic algorithm* (GA) was used as the docking algorithm against ligands Cp1 and Cp2 (Figure 2a) for the rigid blind docking. The grid box in which the interaction was analyzed encapsulated a single monomeric unit of CprB. Except for the number of GA runs, all the default parameters were kept the same for the molecular docking.

Cloning of W185L CprB. The clone of the native protein CprB in the pET26b(+) expression vector was kindly provided to us by Ryo Natsume (Japan Biological Informatics Consortium (JBIC), Tokyo, Japan). A mutant of the original clone was produced by site directed mutagenesis of the Trp-185 to Leu-185, using the primers 5′-CCGGATCAGGATGTACAACATCTCCGCGAGGC-3′ and 5′-GCCTCGCGGAGATGTTGTACATCCTGATCCGG-3′ (primers from IDT, USA) by polymerase chain reaction using the polymerase KAPA HiFi (Kapabiosystems).

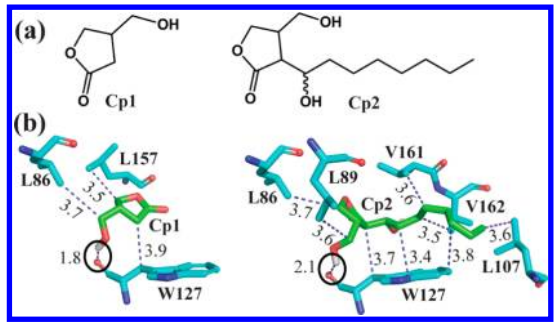

Figure 2. (a) γ-Butyrolactones Cp1 and Cp2 used as quenchers for tryptophan fluorescence quenching studies in CprB. (b) Interactions observed from docking studies of CprB with ligands Cp1 and Cp2. The H-bonding interaction has been circled in black. The distances shown in the figures are in Å.

Purification of Native CprB and Mutant W185L CprB. Plasmids were transformed in BL21(DE3)LysS cells after which the culture was grown in Luria−Bertani broth (Himedia, India) with the antibiotics chloramphenicol and kanamycin at concentrations of 30 and 35 μg/mL, respectively, at 37 °C and 250 rpm. Expression of the protein was induced by the addition of IPTG (isopropyl β-D-1-thiogalactopyranoside from MP Biomedicals, LLC, France) at a concentration of 1 mM when an O.D. of ∼0.6 was attained. The induced cells were cultured for about 3 h at 37 °C and another 3 h at 25 °C before harvesting. The harvested cells were resuspended in a buffer containing 50 mM sodium phosphate, pH 7 (buffer A), followed by homogenization by sonication. Cell debris was removed by centrifugation at 20 000 rpm at 4 °C, and the supernatant was added to SP-sepharose beads (GE Healthcare, WI, US) that had been equilibrated in buffer A. It was then gently stirred on a rocker for 1.5 h. The beads were subsequently separated by centrifugation at 1200 rpm and mounted on a column followed by a slow wash for 6−8 h with buffer A. The protein was further washed with buffers containing 50 mM sodium phosphate and an increasing concentration of NaCl (0.1−0.3 M) and finally eluted with buffer containing NaCl at 0.4 M. The eluted protein was desalted using desalting columns (Econo-Pac10DG columns, Bio-Rad) into a buffer containing 50 mM sodium phosphate pH 7 and 100 mM NaCl and used for fluorescence studies.

Preparation of Ligands Cp1 and Cp2. The detailed discussion for the preparation of the ligands and the scheme followed (Scheme S1) have been provided in the Supporting Information.[27−29]

Fluorescence Measurements. *Steady State Fluorescence Measurements.* Fluorescence measurements were carried out in a Varian Cary Eclipse spectrofluorimeter in a 1 cm path length quartz cuvette at 24 °C. Emission spectra were recorded for wavelength ranging from 305 to 450 nm, for the excitation of the samples at 295 nm. For all the experiments, the protein solution was taken in the cuvette and titrated against the solution of the compounds in a buffer of 50 mM phosphate (pH 7), 100 mM NaCl, and 2% DMSO. Each time,

dx.doi.org/10.1021/jp503589h | J. Phys. Chem. B 2014, 118, 10035−10042

a 5 μL addition of the compound was made to 1 mL of solution of the protein. The samples were incubated for 4−5 min after the addition and mixing of the compound, before recording the emission spectra. All experiments have been repeated at least three times.

Time Resolved Fluorescence Measurements. Time resolved fluorescence experiments were performed on an IBH Horiba-JY fluorocube. The excitation of the 5 μM CprB (in the same buffer system as above) taken in a 1 cm path length quartz cuvette was done at 295 nm by a NanoLED 295 nm (fwhm = 700 ps). The decays were recorded at a magic angle of 54.7°. The data obtained were fitted to the biexponential model by the global reconvolution fitting technique using the software FluoFit (Global Fluorescence Decay Data Analysis Software, Pico Quant, Model no. FluoFit Pro (local)).

Circular Dichroism (CD) Spectroscopy. CD spectra were recorded on a Jasco J-815 CD spectrometer using 3.75 μM protein in phosphate buffer (buffer same as used in fluorescence experiments). Scans were performed at 20 °C using 0.1 cm path length quartz cuvettes with 8 s differential integration time at a scan rate of 50 nm min^{-1}.

Dynamic Light Scattering (DLS) Method. The DLS experiment was performed on a DynaPro-MS800 dynamic light scattering instrument (Protein Solutions Inc., VA) with an inbuilt laser at 820 nm, by monitoring the scattered light at 90° with respect to irradiation direction. The buffer used was the same as that used in the fluorescence experiments. Buffer solutions were filtered to remove dust particles. The protein samples were centrifuged at 6000 rpm before being analyzed to remove any particulate matter that might be present.

RESULTS AND DISCUSSION

Docking Studies of CprB with Ligand Cp1 and Cp2. To date, most of the studies reported with this class of proteins are *in vivo*, performed to ascertain the pathways regulated by these butanolides.[9,17,19] There are also electrophoretic mobility shift assays that have been reported with purified protein to study the effect of the presence and absence of these compounds on DNA binding.[15,19] However, there are no experimental studies confirming the binding of ligands to the pocket situated in the regulatory domain. The X-ray structure of the monomer of CprB in the apo form was used for docking studies to narrow down the plausible ligand binding site and to get insights into the mode of ligand binding. CprB was docked with a spectrum of GBLs containing the basic butyrolactone moiety and those with an appended aliphatic chain at the C2 position varying in length from 5 to 12 carbon atoms. It was observed that chain lengths consisting of more than nine carbon atoms showed a drop in ligand occupancy inside the predicted binding pocket (Table S1, Supporting Information). Compounds with chain lengths of 5−9 carbon atoms were found to be optimal for occupying the cavity.

Figure 2a shows two different GBLs, one with the basic butyrolactone moiety and the other with eight carbon aliphatic chains appended to it. In both cases, the low energy structures showed a similar mode of binding, with the tryptophan residue (W127) interacting with the GBLs via the invariant γ-butyrolactone ring in the proposed regulatory domain. Both ligands exhibited a key hydrogen bonding contact of their respective primary hydroxyl group with the carbonyl oxygen atom of W127 (Figure 2b). This interaction clamps the ligands in an orientation such that the five-membered butyrolactone ring is in close proximity to the W127 residue enabling further interactions with the other residues in the pocket. A large contribution toward the stabilization of the complex is also from the numerous hydrophobic interactions between the ligand and the residues lining the cavity.

Design and Preparation of Ligands. For experimental validation of the results obtained from docking studies, two GBLs were synthesized. The compounds 3-hydroxymethylbutanolide and 2-(1′-hydroxyoctyl)-3-hydroxymethylbutanolide (Cp1 and Cp2, respectively) consist of a common butyrolactone moiety (Figure 2a). Cp1 was designed to estimate the ability of the protein to recognize the basic GBL moiety. The compound Cp2 was designed mimicking the already known GBLs, with an eight-carbon-length aliphatic chain at the C-2 position of the basic Cp1 unit.[10] This compound was synthesized to gauge the requirement of the aliphatic appendage and a secondary hydroxyl group toward selectivity of CprB binding. The synthesis was performed on the basis of the strategy followed earlier for the synthesis of butanolides, and the synthetic scheme followed is described in Scheme S1 (Supporting Information).[27−29]

Ligand Binding Studies. The binding of Cp1 and Cp2 to CprB was investigated by monitoring the tryptophan fluorescence of the protein. The conserved tryptophan residue W127 in the proposed binding pocket, previously shown to be critical for binding,[15] was exploited to sense and report the binding through changes in its fluorescence characteristics. The fluorescence spectra were recorded in the presence of varying concentrations of the ligands, following excitation at 295 nm as depicted in Figure 3a.

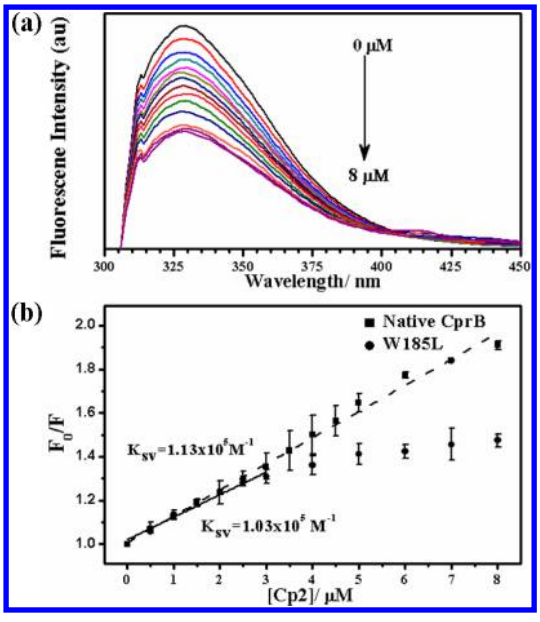

Figure 3. (a) Steady state emission spectra of native CprB protein (3.75 μM) in the presence of varying concentration of Cp2 ligand. (b) Stern−Volmer plot for the native CprB protein and mutant W185L for quenching by the compound Cp2.

The choice of 295 nm for excitation was to minimize the contributions from the five tyrosine and five phenylalanine residues to the emission spectrum. The emission maxima were observed at ∼328 nm, as expected for buried tryptophan residues.[30] The protein concentration used for this study was 3.75 μM. Addition of the compound resulted in fluorescence quenching without any spectral shift. This indicates that the

dx.doi.org/10.1021/jp503589h | J. Phys. Chem. B 2014, 118, 10035−10042

local environment of the tryptophan residue is not altered upon interaction with the ligand. The fluorescence data collected was analyzed with the Stern–Volmer (SV) equation, using the fluorescence intensity at spectral maxima (Figure 3b).[31−34] Analysis of quenching data for both Cp1 and Cp2 resulted in almost identical K_{SV} values (Table 1).

Table 1. Stern–Volmer Constants (K_{SV}) for Quenching Titrations of Native CprB and W185L Mutant Protein with Ligands Cp1 and Cp2, at Various Concentrations of Protein

protein	[protein] (μM)	compound	K_{SV} (10^5 M^{-1})
CprB	1.50	Cp1	3.44 ± 0.56
CprB	3.75	Cp1	1.37 ± 0.26
CprB	7.50	Cp1	0.47 ± 0.06
CprB	1.50	Cp2	2.95 ± 0.37
CprB	3.75	Cp2	1.13 ± 0.18
CprB	7.50	Cp2	0.31 ± 0.04
W185L CprB	3.75	Cp1	0.75 ± 0.04
W185L CprB	7.50	Cp1	0.34 ± 0.04
W185L CprB	3.75	Cp2	1.03 ± 0.08
W185L CprB	7.50	Cp2	0.31 ± 0.05

The K_{SV} values, which represent the binding affinity between the quencher and fluorophore, indicate that, in terms of specificity of binding, both Cp1 and Cp2 show significant similarity. This is in agreement with the docking studies mentioned earlier in this article, which clearly showed that the mode of binding of the two compounds was similar. Hence, it can be concluded that the major contribution to the fluorescence quenching is due to the interaction of the butyrolactone ring, common in both compounds with the tryptophan residing in the pocket.

The quenching experiments were repeated with the mutant W185L, in which the tryptophan away from the binding pocket was mutated to the nonfluorescent leucine residue. This was done to delineate the contribution toward fluorescence quenching of this tryptophan residue (W185) from the tryptophan residue of interest (W127). The Stern–Volmer plot for the mutant was linear for lower concentrations of Cp2 but exhibited a distinct saturation at concentrations above 3.5 μM, which is approximately the same concentration as the protein (Figure 3b). The slope (K_{SV}) in the linear region is similar to that of the native protein, indicating that Cp2 binds equally well to the cavity (Table 1), resulting in quenching of tryptophan fluorescence. This observation reconfirms the docking results and proves that only W127 is affected by the ligand binding to CprB. The deviation from linearity at higher ligand concentration possibly arises due to the changes in protein structure in the presence of excess ligand or an increase in nonspecific binding with the ligand. A deviation from the linear Stern–Volmer plot was also observed in the native protein though at a much higher ligand concentration (Figures S1 and S2, Supporting Information). Additionally, it was observed during purification that W185L was more prone to proteolysis than the wild type protein. This observation further rationalizes the nonlinear behavior observed at a lower concentration in the case of the mutant protein, as its secondary structure appears to be more prone to perturbation. The removal of the tryptophan residue has possibly introduced instability in the protein, an effect which has been previously observed in other systems as well.[35]

Time resolved fluorescence studies were carried out to ascertain whether the observed quenching is static/dynamic in nature. The time-resolved fluorescence decay curves were recorded for CprB in the absence and presence of Cp2 ligand with increasing concentrations (Figure 4). All the fluorescence decay curves were fitted by global analysis, and the results are listed in Table 2.

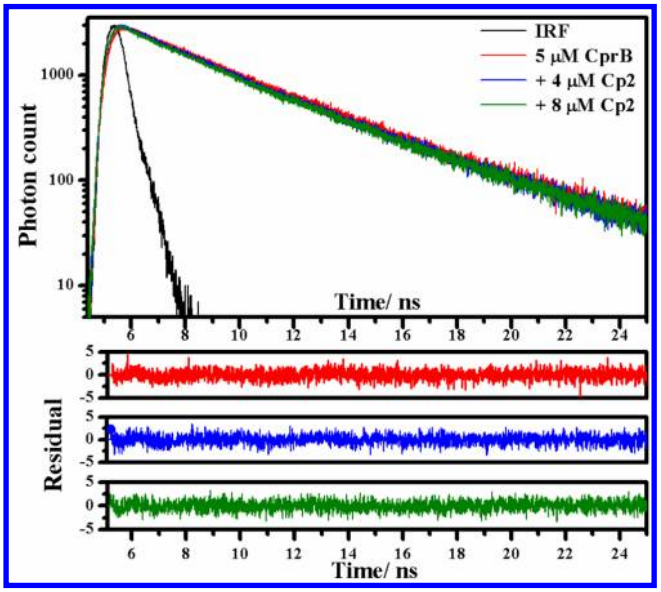

Figure 4. Time resolved fluorescence decay curve for native CprB (5 μM) and complexes with Cp2 (4 and 8 μM). The respective residual plots for the fitting are represented below.

Table 2. Time Resolved Fluorescence Measurement Data of Native CprB Protein (5 μM) in the Presence of Varying Cp2 Concentrations

[Cp2] (μM)	α_1	α_2	τ_1 (ns)	τ_2 (ns)	mean τ (ns)	χ^2
0	0.69	0.31	4.76	2.56	4.08	1.04
1.0	0.69	0.31	4.76	2.56	4.08	1.07
2.0	0.65	0.35	4.76	2.56	3.99	1.05
4.0	0.65	0.35	4.76	2.56	3.99	1.03
6.0	0.65	0.35	4.76	2.56	3.99	1.02
8.0	0.68	0.32	4.76	2.56	4.06	1.05
10.0	0.66	0.34	4.76	2.56	4.01	1.07

All the fluorescence decay curves could be fitted to a biexponential function. The presence of two lifetimes can be attributed to slightly different environments experienced by the two tryptophan residues and/or by the existence of multiple conformations of each tryptophan.[36−39] Assuming that the tryptophan residues are structurally rigid, the individual lifetimes will reflect the local environment.[40] Structural analysis shows that both of the tryptophan residues are surrounded by hydrophobic residues. W185, which is in a densely packed environment and closer to the surface, most likely has the shorter lifetime τ_2, whereas W127 that resides in a deep pocket plausibly possesses the longer lifetime τ_1. More importantly, it was observed that the tryptophan fluorescence lifetimes do not change with the addition of Cp2, which clearly signifies static quenching. The X-ray structure reveals that W185 is completely surrounded by other amino acid residues with no space for either of the GBLs to come in close proximity to interact with it. Hence, on account of the facts that there is no change in

dx.doi.org/10.1021/jp503589h | J. Phys. Chem. B 2014, 118, 10035−10042

lifetime of the W185 and that both the native and W185L mutant versions of the proteins exhibit similar K_{SV} values, we can conclude that W185 does not contribute toward ligand binding.

In order to ascertain the extent of exposure of the tryptophan moieties to the surface, fluorescence quenching experiments were carried out using KI.[41−44] It was observed that only 12% of the CprB (1.5 μM) fluorescence was quenched by 20 μM KI (Figure 5).

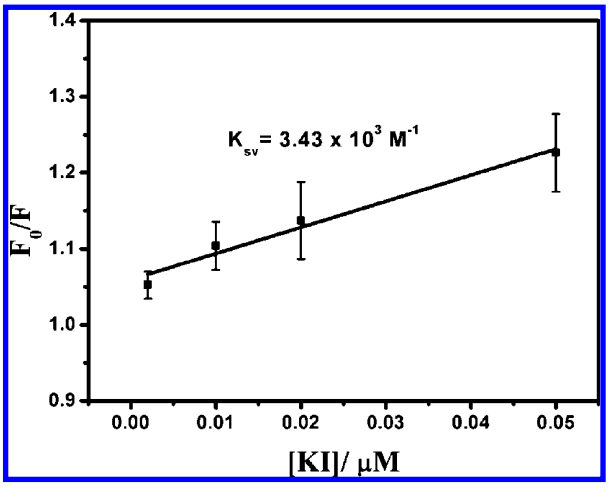

Figure 5. Stern−Volmer plot for KI quenching of CprB (1.5 μM).

These results clearly confirm that both of the tryptophan residues are buried and not accessible to the surface quencher KI. K_{SV} for quenching by KI (3.43×10^3 M^{-1}) is approximately 2 orders below that for the ligand quenching (Table 1), indicating the higher accessibility of the tryptophan residues to the ligands as compared to KI.

To investigate the changes in the secondary structure of the protein upon addition of ligand Cp2, circular dichroism (CD) spectroscopy was performed at the far UV region. The CD spectrum of CprB shows the characteristic bands of α-helix at 208 and 222 nm for the native protein, which is consistent with the crystal structure of CprB (Figure 6).[45] The spectrum of the protein shows marginal changes in the presence of nearly equivalent ligand concentrations. This indicates that the integrity of the protein structure is not destroyed upon addition of ligand in the 1:1 ratio. However, a 3-fold increase in the ligand concentration leads to a discernible change in the intensity, though the nature of the spectrum remains unchanged.

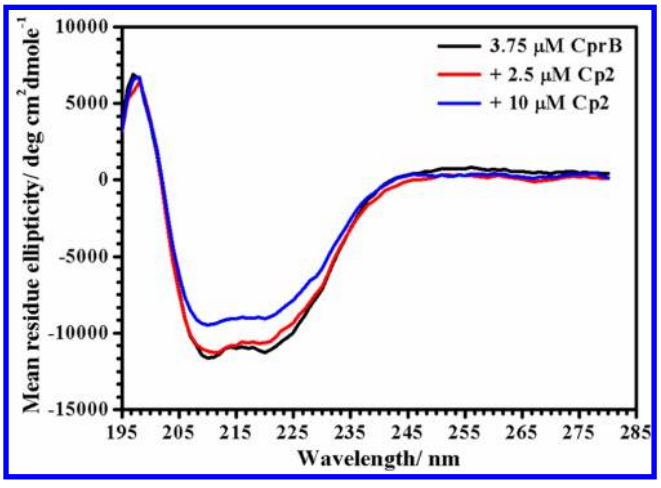

Figure 6. CD spectra for CprB protein at a concentration of 3.75 μM and with compound Cp2 at concentrations of 2.5 and 10 μM.

This suggests that, in the presence of 10 μM Cp2, CprB maintains the helix pattern similar to that observed for the native protein. The partial loss of helical structure is attributed to the presence of excess ligand. Since under physiological conditions these GBLs are effective at low concentrations, our studies in the lower micromolar range of concentration should suffice to deduce information pertaining to the ligand binding.

Concentration Dependence of K_{SV}. The tryptophan quenching experiments were performed for three different concentrations of the native protein, 1.5, 3.75, and 7.5 μM in the ratio 2:5:10 for both the compounds Cp1 and Cp2 (plots of tryptophan emission quenching in individual experiments and their extended Stern−Volmer plots are provided in the Supporting Information, Figures S1 and S2). A comparison between the slopes of the Stern−Volmer plots at different protein concentrations showed a distinct dependence on concentration (Figure 7).

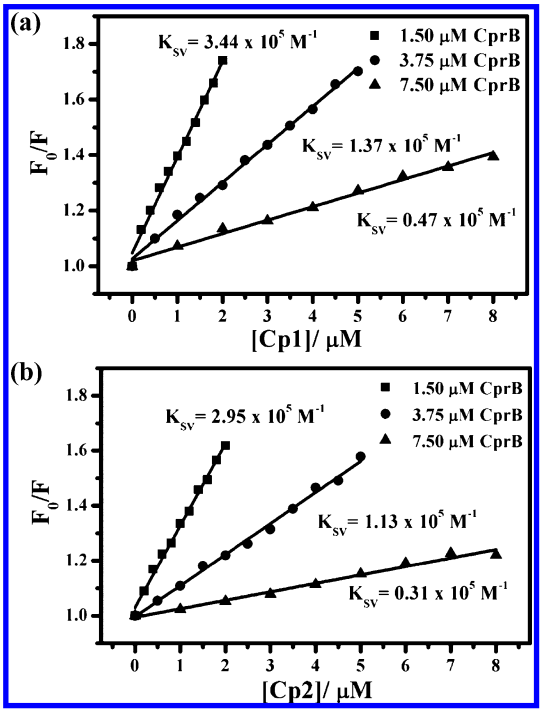

Figure 7. Stern−Volmer plots for the native CprB at concentrations of 1.50, 3.75, and 7.50 μM with compounds Cp1 (a) and Cp2 (b) with average standard deviations of 4.6 and 3.4%, respectively, of F_0/F. Figure S5 (Supporting Information) is a duplicate figure showing the individual error bars.

With the increase in concentration of the protein, there was a significant drop in the value of the binding constant K_{SV}. For the compound Cp1, the value of the Stern−Volmer constant decreases by 60% for a 2.5-fold increase in protein concentration (1.5 to 3.75 μM) and an additional 66% decrease for a further 2-fold increase (3.75 to 7.5 μM). For Cp2, the same trend was prevalent with the initial fall of 62% for the 2.5-fold increase in protein concentration and a decrease by 72% for the 2-fold increase (Table 1). A similar concentration dependence of K_{SV} was also observed in the W185L mutant for

dx.doi.org/10.1021/jp503589h | J. Phys. Chem. B 2014, 118, 10035−10042

both compounds (Table 1; Figures S3 and S4, Supporting Information). The cause of this trend could be attributed to the tendency of the protein to oligomerize.[23] The property of oligomerization, which is known to be a concentration dependent effect, could be the reason behind the inefficient binding of the compounds with the increased protein concentration, thereby resulting in a decreased binding constant as depicted in Figure 7.

To confirm the oligmerization tendency, dynamic light scattering (DLS) experiments were performed with the protein at various concentrations. The lowest possible concentration that can be used to obtain a sufficient signal was 3.75 μM. An increase in the hydrodynamic radius from 2.69 to 3.24 nm was observed as the concentration increased from 3.75 to 25 μM (Figure 8).

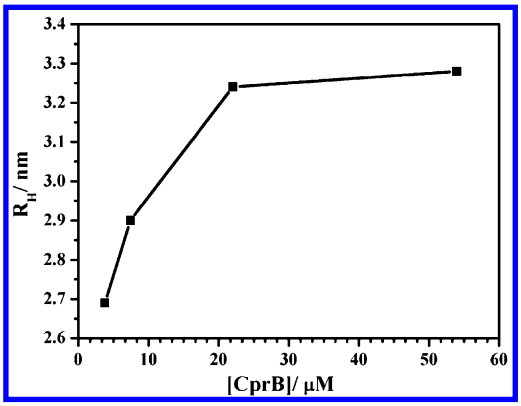

Figure 8. Variation of hydrodynamic radius of native CprB as a function of protein concentration obtained from DLS experiments. The standard deviation for each value of radius was below 6%.

Though the increase in hydrodynamic radius is not indicative of large scale oligomerization, there is a definite indication for protein forming multimers in the solution as a function of protein concentration. The hydrodynamic radius is known to increase as the cube root of the aggregation for nearly spherical aggregates. The percentage increase in the hydrodynamic radius is thus approximately equivalent to doubling of the size of the protein. This oligomerization, therefore, can cause a hindrance to the ligand binding in the buried cavity, as indicated by the drop in K_{SV} values. These results pertaining to concentration dependent changes in binding provide important insights into the choice of optimal concentrations for GBL screening. It can be concluded that effective measurements of ligand binding are best when performed at lower protein concentrations where protein aggregation is less, thereby providing a better accessibility to the ligand.

CONCLUSIONS

CprB is the only protein among the various known GBL-binding receptors of the *Streptomyces* species whose structure has been solved. As reported, CprB possesses two functional domains, the regulatory and the DNA binding domain. Our interest has lied in the regulatory domain where the structure specifically shows a pocket for ligand binding. Since the specific ligand for the protein has not yet been identified, attempts have been made to narrow down the ligand structure and the method to monitor such a process. The presence of a conserved tryptophan residue in the pocket enabled the monitoring of the ligand binding through fluorescence quenching. The binding of two synthetic GBLs was investigated for the native protein and its W185L mutant. The binding of the GBLs leads to fluorescence quenching in both the native protein and its W185L mutant. The fluorescence quenching studies on the W185L mutant clearly establish the fact that both of the GBLs (Cp1 and Cp2) bind in the ligand binding pocket. Similar K_{SV} values observed for both Cp1 and Cp2 ligands assisted in the conclusion that the γ-butyrolactone ring is primarily contributing to quenching. Further, it was observed that the binding of the γ-butyrolactones is dependent on the protein concentration, which can be attributed to the oligomerization tendency of the protein.

ASSOCIATED CONTENT

Supporting Information

Percentage occupancy of pocket by ligand from docking studies, scheme and synthetic details for ligand preparation, and NMR of products. Additionally, Stern–Volmer plots for individual experiments showing the slope of the initial linear stretch of the plot and their individual fluorescence quenching shown as an inset are provided. This material is available free of charge via the Internet at http://pubs.acs.org.

AUTHOR INFORMATION

Corresponding Authors

*E-mail: naresh@chem.iitb.ac.in.
*E-mail: ruchi@chem.iitb.ac.in.

Present Address

‡(B.H.) IITB-Monash Research Academy, Indian Institute of Technology Bombay, Mumbai, Maharashtra 400076, India

Notes

The authors declare no competing financial interest.

ACKNOWLEDGMENTS

The authors would like to thank Prof. Anindya Dutta (IIT Bombay, Mumbai) for assistance with the time-resolved fluorescence experiments as well helpful suggestions. The authors are also grateful to Prof. G. Krishnamoorthy (TIFR, Mumbai) for his invaluable suggestions and for providing the facility for DLS experiments. This work was supported by IIT Bombay, CSIR (for fellowship of A. Biswas), DBT (BT/PRI3766/BRB/10/785/2010) and DST (SR/S/BB-53/2010).

REFERENCES

(1) Bassler, B. L.; Losick, R. Bacterially Speaking. *Cell* **2006**, *125*, 237–246.
(2) Visick, K. L.; Fuqua, C. Decoding Microbial Chatter: Cell-cell Communication in Bacteria. *J. Bacteriol.* **2005**, *187*, 5507–5519.
(3) Fuqua, C.; Winans, S. C.; Greenberg, E. P. Census and Consensus in Bacterial Ecosystems: The LuxR-LuxI Family of Quorum-sensing Transcriptional Regulators. *Annu. Rev. Microbiol.* **1996**, *50*, 727–751.
(4) Camilli, A.; Bassler, B. L. Bacterial Small-molecule Signaling Pathways. *Science* **2006**, *311*, 1113–1116.
(5) Déziel, E.; Gopalan, S.; Tampakaki, A. P.; Lépine, F.; Padfield, K. E.; Saucier, M.; Xiao, G.; Rahme, L. G. The Contribution of MvfR to *Pseudomonas aeruginosa* Pathogenesis and Quorum Sensing Circuitry Regulation: Multiple Quorum Sensing-regulated Genes are Modulated Without Affecting *lasRI*, *rhlRI* or the Production of N-acyl-L-homoserine Lactones. *Mol. Microbiol.* **2005**, *55*, 998–1014.
(6) Fuqua, C.; Greenberg, E. P. Listening in on Bacteria: Acyl-homoserine Lactone Signalling. *Nat. Rev. Mol. Cell Biol.* **2002**, *3*, 685–695.

(7) Déziel, E.; Lépine, F.; Milot, S.; He, J.; Mindrinos, M. N.; Tompkins, R. G.; Rahme, L. G. Analysis of *Pseudomonas aeruginosa* 4-hydroxy-2-alkylquinolines (HAQs) Reveals a Role for 4-hydroxy-2-heptylquinoline in Cell-to-cell Communication. *Proc. Natl. Acad. Sci. U. S. A.* **2004**, *101*, 1339−1344.
(8) Pesci, E. C.; Milbank, J. B. J.; Pearson, J. P.; McKnight, S.; Kende, A. S.; Greenberg, E. P.; Iglewski, B. H. Quinolone Signaling in the Cell-to-cell Communication System of *Pseudomonas aeruginosa*. *Proc. Natl. Acad. Sci. U. S. A.* **1999**, *96*, 11229−11234.
(9) Hsiao, N. H.; Nakayama, S.; Merlo, M. E.; de Vries, M.; Bunet, R.; Kitani, S.; Nihira, T.; Takano, E. Analysis of Two Additional Signaling Molecules in *Streptomyces coelicolor* and the Development of a Butyrolactone-specific Reporter System. *Chem. Biol.* **2009**, *16*, 951−960.
(10) Takano, E. Gamma-butyrolactones: Streptomyces Signalling Molecules Regulating Antibiotic Production and Differentiation. *Curr. Opin. Microbiol.* **2006**, *9*, 287−294.
(11) Pottathil, M.; Lazazzera, B. A. The Extracellular Phr Peptide-Rap Phosphatase Signaling Circuit of *Bacillus subtilis*. *Front. Biosci.* **2003**, *8*, d32−d45.
(12) Holden, M. T.; Ram, C. S.; de Nys, R.; Stead, P.; Bainton, N. J.; Hill, P. J.; Manefield, M.; Kumar, N.; Labatte, M.; England, D.; et al. Quorum-sensing Cross Talk: Isolation and Chemical Characterization of Cyclic Dipeptides from *Pseudomonas aeruginosa* and other Gram-negative Bacteria. *Mol. Microbiol.* **1999**, *33*, 1254−1266.
(13) Khokhlov, A. S.; Tovarova, I. I.; Borisova, L. N.; Pliner, S. A.; Shevchenko, L. N.; Kornitskaia, E. I.; Ivkina, N. S.; Rapoport, I. A. The A-factor, Responsible for Streptomycin Biosynthesis by Mutant Strains of *Actinomyces streptomycini*. *Dokl. Akad. Nauk SSSR* **1967**, *177*, 232−235.
(14) Horinouchi, S. A Microbial Hormone, A-factor, as a Master Switch for Morphological Differentiation and Secondary Metabolism in *Streptomyces griseus*. *Front. Biosci.* **2002**, *7*, d2045−d2057.
(15) Sugiyama, M.; Onaka, H.; Nakagawa, T.; Horinouchi, S. Site-directed Mutagenesis of the A-factor Receptor Protein: Val-41 Important for DNA-binding and Trp-119 Important for Ligand-binding. *Gene* **1998**, *222*, 133−144.
(16) Onaka, H.; Ando, N.; Nihira, T.; Yamada, Y.; Beppu, T.; Horinouchi, S. Cloning and Characterization of the A-factor Receptor Gene from *Streptomyces griseus*. *J. Bacteriol.* **1995**, *177*, 6083−6092.
(17) Horinouchi, S.; Beppu, T. A-factor as a Microbial Hormone that Controls Cellular Differentiation and Secondary Metabolism in *Streptomyces griseus*. *Mol. Microbiol.* **1994**, *12*, 859−864.
(18) Kinoshita, H.; Ipposhi, H.; Okamoto, S.; Nakano, H.; Nihira, T.; Yamada, Y. Butyrolactone Autoregulator Receptor Protein (BarA) as a Transcriptional Regulator in Streptomyces virginiae. *J. Bacteriol.* **1997**, *179*, 6986−6993.
(19) Takano, E.; Chakraburtty, R.; Nihira, T.; Yamada, Y.; Bibb, M. J. A Complex Role for the γ-butyrolactone SCB1 in Regulating Antibiotic Production in *Streptomyces coelicolor* A3(2). *Mol. Microbiol.* **2001**, *41*, 1015−1028.
(20) Waki, M.; Nihira, T.; Yamada, Y. Cloning and Characterization of the Gene (farA) Encoding the Receptor for an Extracellular Regulatory Factor (IM-2) from Streptomyces sp. Strain FRI-5. *J. Bacteriol.* **1997**, *179*, 5131−5137.
(21) Kitani, S.; Kinoshita, H.; Nihira, T.; Yamada, Y. In Vitro Analysis of the Butyrolactone Autoregulator Receptor Protein (FarA) of *Streptomyces lavendulae* FRI-5 Reveals that FarA Acts as a DNA-Binding Transcriptional Regulator that Controls its Own Synthesis. *J. Bacteriol.* **1999**, *181*, 5081−5084.
(22) Onaka, H.; Nakagawa, T.; Horinouchi, S. Involvement of Two A-factor Receptor Homologues in *Streptomyces coelicolor* A3(2) in the Regulation of Secondary Metabolism and Morphogenesis. *Mol. Microbiol.* **1998**, *28*, 743−753.
(23) Natsume, R.; Takeshita, R.; Sugiyama, M.; Ohnishi, Y.; Senda, T.; Horinouchi, S. Crystallization of CprB, an Autoregulator-receptor Protein from *Streptomyces coelicolor* A3(2). *Acta Crystallogr., Sect. D* **2003**, *59*, 2313−2315.
(24) Natsume, R.; Ohnishi, Y.; Senda, T.; Horinouchi, S. Crystal Structure of a Gamma-butyrolactone Autoregulator Receptor Protein in *Streptomyces coelicolor* A3(2). *J. Mol. Biol.* **2004**, *336*, 409−419.
(25) Ramos, J. L.; Martinez-Bueno, M.; Molina-Henares, A. J.; Terán, W.; Watanabe, K.; Zhang, X.; Gallegos, M. T.; Brennan, R.; Tobes, R. The TetR Family of Transcriptional Repressors. *Microbiol. Mol. Biol. Rev.* **2005**, *69*, 326−356.
(26) Morris, G. M.; Huey, R.; Lindstrom, W.; Sanner, M. F.; Belew, R. K.; Goodsell, D. S.; Olson, A. J. AutoDock4 and AutoDockTools4: Automated Docking with Selective Receptor Flexibility. *J. Comput. Chem.* **2009**, *30*, 2785−2791.
(27) Weber, W.; Schoenmakers, R.; Spielmann, M.; El-Baba, M. D.; Folcher, M.; Keller, B.; Weber, C. C.; Link, N.; van de Wetering, P.; Heinzen, C.; et al. Streptomyces-derived Quorum-sensing Systems Engineered for Adjustable Transgene Expression in Mammalian Cells and Mice. *Nucleic Acids Res.* **2003**, *31*, e71.
(28) Takano, E.; Nihira, T.; Hara, Y.; Jones, J. J.; Gershater, C. J.; Yamada, Y.; Bibb, M. Purification and Structural Determination of SCB1, a Gamma-butyrolactone that Elicits Antibiotic Production in *Streptomyces coelicolor* A3(2). *J. Biol. Chem.* **2000**, *275*, 11010−11016.
(29) Yamada, Y.; Sugamura, K.; Kondo, K.; Yanagimoto, M.; Okada, H. The Structure of Inducing Factors for Virginiamycin Production in *Streptomyces virginiae*. *J. Antibiot.(Tokyo)* **1987**, *40*, 496−504.
(30) Konev, S. V. *Fluorescence and Phosphorescence of Proteins and Nucleic Acids*; Plenum Press: New York, 1967.
(31) Papadopoulou, A.; Green, R. J.; Frazier, R. A. Interaction of Flavonoids with Bovine Serum Albumin: A Fluorescence Quenching Study. *J. Agric. Food Chem.* **2004**, *53*, 158−163.
(32) Sukowska, A. Interaction of Drugs with Bovine and Human Serum Albumin. *J. Mol. Struct.* **2002**, *614*, 227−232.
(33) Sonveaux, N.; Vigano, C.; Shapiro, A. B.; Ling, V.; Ruysschaert, J. M. Ligand-mediated Tertiary Structure Changes of Reconstituted P-glycoprotein: A Tryptophan Fluorescence Quenching Analysis. *J. Biol. Chem.* **1999**, *274*, 17649−17654.
(34) Chadborn, N.; Bryant, J.; Bain, A. J.; O'Shea, P. Ligand-dependent Conformational Equilibria of Serum Albumin Revealed by Tryptophan Fluorescence Quenching. *Biophys. J.* **1999**, *76*, 2198−2207.
(35) James, N. G.; Byrne, S. L.; Steere, A. N.; Smith, V. C.; Mac Gillivray, R. T.; Mason, A. B. Inequivalent Contribution of the Five Tryptophan Residues in the C-Lobe of Human Serum Transferrin to the Fluorescence Increase when Iron is Released. *Biochemistry* **2009**, *48*, 2858−2867.
(36) Beechem, J. M.; Brand, L. Time-Resolved Fluorescence of Proteins. *Annu. Rev. Biochem.* **1985**, *54*, 43−71.
(37) Engh, R. A.; Chen, L. X. Q.; Fleming, G. R. Conformational Dynamics of Tryptophan: A Proposal for the Origin of the Non-exponential Fluorescence Decay. *Chem. Phys. Lett.* **1986**, *126*, 365−372.
(38) Petrich, J. W.; Chang, M. C.; McDonald, D. B.; Fleming, G. R. On the Origin of Nonexponential Fluorescence Decay in Tryptophan and its Derivatives. *J. Am. Chem. Soc.* **1983**, *105*, 3824−3832.
(39) Chang, M. C.; Petrich, J. W.; McDonald, D. B.; Fleming, G. R. Nonexponential Fluorescence Decay of Tryptophan, Tryptophylglycine, and Glycyltryptophan. *J. Am. Chem. Soc.* **1983**, *105*, 3819−3824.
(40) Rouviere, N.; Vincent, M.; Craescu, C. T.; Gallay, J. Immunosuppressor Binding to the Immunophilin FKBP59 Affects the Local Structural Dynamics of a Surface β-strand: Time-resolved Fluorescence Study. *Biochemistry* **1997**, *36*, 7339−7352.
(41) Lehrer, S. S. Solute Perturbation of Protein Fluorescence. Quenching of the Tryptophyl Fluorescence of Model Compounds and of Lysozyme by Iodide Ion. *Biochemistry* **1971**, *10*, 3254−3263.
(42) Lakshmikanth, G. S.; Krishnamoorthy, G. Solvent-exposed Tryptophans Probe the Dynamics at Protein Surfaces. *Biophys. J.* **1999**, *77*, 1100−1106.
(43) Pawagi, A. B.; Deber, C. M. Ligand-dependent Quenching of Tryptophan Fluorescence in Human Erythrocyte Hexose Transport Protein. *Biochemistry* **1990**, *29*, 950−955.

(44) Hansen, D.; Altschmied, L.; Hillen, W. Engineered Tet Repressor Mutants with Single Tryptophan Residues as Fluorescent Probes. Solvent Accessibilities of DNA and Inducer Binding Sites and Interaction with Tetracycline. *J. Biol. Chem.* **1987**, *262*, 14030−14035.
(45) Holzwarth, F.; Doty, P. The Ultraviolet Circular Dichroism of Polypeptides. *J. Am. Chem. Soc.* **1965**, *87*, 218−228.

Supporting Information

Fluorescence Quenching Studies of γ-Butyrolactone Binding Protein (CprB) from *Streptomyces coelicolor* A3(2)

Anwesha Biswas, Ravi K. Swarnkar, Bhukya Hussain, Suraj K. Sahoo, P. I. Pradeepkumar, G. Naresh Patwari,* Ruchi Anand*

Department of Chemistry, Indian Institute of Technology Bombay, Mumbai, Maharashtra 400076, India

Details of docking studies in terms of percentage occupancy of pocket by ligand have been provided. The scheme and synthetic details for ligand preparation and NMR of respective products have also been included. Additionally, Stern-Volmer plots for individual experiments showing slope of the initial linear stretch of the plot and their individual fluorescence quenching (inset) have been provided. Stern-Volmer plots of the main paper have also been shown here along with the error bars.

Results from docking studies of CprB and GBLs, with varying aliphatic chain length

Table S1. Table showing the percentage of ligand occupancy within the proposed ligand binding pocket for the respective GBL with the specified length of aliphatic chain at C2, from docking studies.

Carbon chain length	Percentage occupancy outside ligand binding pocket
5	10.8
6	10
7	0
8	21.6
9	21.2
10	37.2
11	46.2
12	62.8

Preparation of ligands Cp1 and Cp2

The preparation of ligands Cp1 and Cp2 has been achieved using reported procedures[1-3] as shown in Scheme S1. Diethyl succinate was subjected to formylation with ethyl formate and NaH in diethyl ether to yield aldehyde product **1** in 51.3% yield.[1,2] $NaBH_4$ reduction of aldehydic group in **1** followed by condensation and hydrolysis resulted in **Cp1** in 13.9% yield.[1,2] TMS protection of the hydroxyl group in **Cp1** followed by acylation with heptanoyl chloride gave the corresponding keto compound.[1,2] TMS deprotection followed by $NaBH_4$ reduction of keto group gave **Cp2** in 21.4% yield.[2,3]

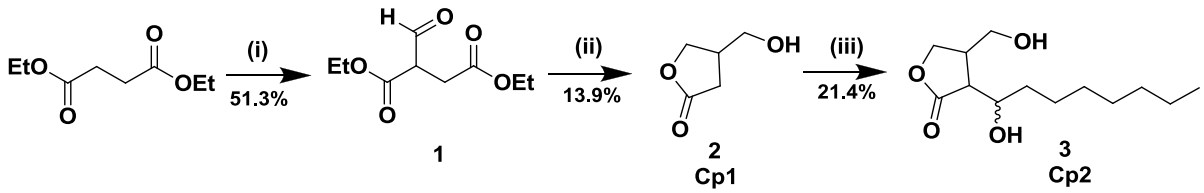

Scheme S1. Preparation of ligands **Cp1** and **Cp2**. Reaction conditions: (i) NaH, HCOOEt, Et_2O, RT, 15 h; (ii) **a**. $NaBH_4$ with ice cooling, EtOH, RT, 3 h. **b**. K_2CO_3, MeOH and water, reflux, 3 h; (iii) **a**. TMSCl, HMDS, pyridine, RT, 2 h. **b**. LDA, THF, –78°C, heptanoyl chloride, 3 h. **c.** EtOH-H_2O, reflux. **d.** $NaBH_4$, MeOH, 0°C, 2h.

General notes

All chemicals and dry solvents (THF) were commercially obtained and used without any further purification. Pyridine was dried over calcium hydride. ^{1}H NMR and ^{13}C NMR were recorded in Bruker Avance III 400 spectrometer. The chemical shifts (δ) are reported in parts per million (ppm) relative to $CDCl_3$ 7.26 ppm and 77.23 ppm for ^{1}H NMR and ^{13}C NMR spectra respectively. Multiplicities of ^{1}H NMR spin couplings are reported as singlet (s), doublet (d), triplet (t), quartet (q), doublet of doublet (dd), quartet of doublet (qd) and multiplet (m). The coupling constants (*J*) are reported in Hz. Silica gel plates precoated with fluorescent indicator were used for performing thin layer chromatography (TLC). Silica gel (100-200 mesh) was used for carrying out purification by column chromatography. MS-ESI(+) was performed with Q-TOF analyzer.

Experimental details

Diethyl formyl succinate (1)

To a stirred solution of NaH (2.75 g, 114 mmol) in 75 mL of diethyl ether, a mixture of diethyl succinate (20 g, 114 mmol), ethyl formate (10.2 g, 138 mmol) and 20 mL ethanol was added at room temperature and stirring was continued for 5 h. The resulting reaction mixture was left overnight. Then, 50 mL water was added to the reaction mixture and the aqueous phase was acidified using 2 M HCl followed by washing with brine solution and subsequent extraction with diethyl ether (3 × 150 mL). The ether extract was then dried over Na_2SO_4, filtered and concentrated. The remaining liquid was distilled under vacuum (bp 76 °C/6 mbar), resulting in a colorless oil (12 g, 51.3%) to yield compound **1**. R_f = 0.3 (33% ethyl acetate in hexane); ^{1}H NMR (400 MHz, $CDCl_3$), δ: 11.52 (d, J = 12.6 Hz, 1H), 7.08 (d, J = 12.7 Hz, 1H), 4.29-4.20 (m, 4H), 2.89 (qd, J = 14.7, 6.1 Hz, 2H), 1.30 (t, J = 7.1 Hz, 6H); MS-ESI(+): Calculated for $C_9H_{15}O_5$ $[M+H]^+$ 203.09; found 203.09.

3-hydroxymethylbutanolide (Cp1)

$NaBH_4$ (1.01 g, 26 mmol) was added stepwise to an ice cold solution of **1** (5 g, 24 mmol) in 20 mL ethanol under stirring. Then the reaction mixture was stirred for 3 h at room temperature. 4 M aqueous HCl solution was added and the solution was stirred further for 1 h. The precipitate formed was filtered off. The filtrate was concentrated and the residue was extracted with ethyl acetate. The organic solution was washed with brine, dried over Na_2SO_4 and concentrated to give 2 g of yellowish oil. The oil was dissolved in a mixture of 12 mL methanol and 4 mL water and then K_2CO_3 (1.5 g) was added to it in small portions. The mixture was then refluxed for 3 h followed by acidification with 4 M HCl and concentrated. The residue was extracted with ethyl acetate (3 × 125 mL) and the organic solution was washed with brine, dried over Na_2SO_4 and concentrated. The product was purified by column chromatography (10% DCM in methanol) resulting in the pure lactone **Cp2** (0.4 g, 21%). R_f = 0.53 (5% ethanol in ethyl acetate); ^{1}H NMR (400 MHz, $CDCl_3$), δ: 4.41 (dd, J = 9.3, 7.5 Hz, 1H), 4.22 (dd, J = 9.3, 5.3 Hz, 1H), 3.71-3.62 (m, 2H), 2.80-2.73 (m, 1H), 2.61 (dd, J = 17.7, 8.9 Hz, 1H), 2.39 (dd, J = 17.7, 5.9 Hz, 1H); ^{13}C-NMR (100 MHz; $CDCl_3$), δ: 177.8, 70.9, 63.1, 37.2, 31.1; MS-ESI(+): Calculated for $C_5H_9O_3$ $[M+H]^+$ 117.0547; found 117.0552.

2-(1'-hydroxyoctyl)-3-hydroxymethylbutanolide (Cp2)

Hexamethyldisilazane (0.09 mL, 0.40 mmol) and trimethylsilyl chloride (0.08 mL, 0.62 mmol) were added to an ice-cooled solution of **Cp1** (60 mg, 0.52 mmol) in 2 mL pyridine, and the reaction mixture was and stirred for 2 h at room temperature under a nitrogen atmosphere resulting in the formation of white precipitate. Then, 5 mL of benzene/hexane (1:1 v/v) was added to the reaction mixture and the precipitate was removed by filtration. The filtrate was concentrated and the crude material subjected to column chromatography (33% ethyl acetate in hexane) to produce a yellowish oily product (78 mg).

The oily compound was dissolved in 3 mL of THF and added to LDA solution [prepared by using N,N-diisopropylamine (0.145 mL, 1.06 mmol) and n-butyl lithium (0.65 mL, 1.06 mmol, 1.6 M in hexane) at –78 °C followed by stirring for 15 min]. To this mixture heptanoyl chloride (60 mg, 0.41 mmol), was added and the reaction was stirred for another 1.5 h, at –78 °C. The reaction mixture was allowed to warm up to 0 °C followed by the addition of 10 mL ice-cold water with 1.5 mL acetic acid. The product formed was subsequently extracted with dichloromethane (3 × 100 mL) and concentrated. The residue was dissolved in 200 mL dichloromethane, washed with 100 mL saturated aq. $NaHCO_3$ and brine. After removal of the solvents, the silyl protected compound was obtained as yellowish oil. The trimethylsilyl group was removed by refluxing with 10 mL of ethanol and 4 mL of water for 30 min. After concentrating, the resulting mixture was purified by column chromatography (20-33% ethyl acetate in hexane) to yield 2-(octanoyl)-3-hydroxymethylbutanolide (50 mg, 0.2 mmol) as an oily liquid.

The compound was dissolved in 8 mL of ethanol and $NaBH_4$ (10.5 mg, 0.3 mol) was added at 0 °C with stirring for 3 h followed by the addition of 3 M aqueous HCl solution. The precipitate formed was removed by filtration and the aqueous solution was extracted with ethyl acetate (3 × 50 mL) and the organic extract was dried over Na_2SO_4. The compound was purified by HPLC to obtain **Cp2** in 21.4% yield (27.73 mg). R_f = 0.32 (33% ethyl acetate in hexane); ^{1}H NMR (400 MHz, $CDCl_3$), δ: 4.23-4.13 (m, 2H), 3.96-3.91 (m, 1H), 3.70 (dd, J = 11.4, 4.0 Hz, 1H), 3.60 (dd, J = 11.5, 5.7 Hz, 1H), 3.19-3.11 (m, 1H), 2.35 (t, J = 7.6 Hz, 1H), 1.67 (m), 1.25 (m), 0.88 (t, J = 6.8 Hz, 3H); ^{13}C-NMR (100 MHz; $CDCl_3$), δ: 70.5, 65.4, 63.6, 34.4, 32.2, 29.67, 29.58, 29.47, 29.35, 25.1, 22.9, 14.3; MS-ESI(+): Calculated for $C_{13}H_{25}O_4$ $[M+H]^+$ 245.1753; found 245.1754.

Stern-Volmer plots of individual experiments with fluorescence intensity quenching spectra provided inset.

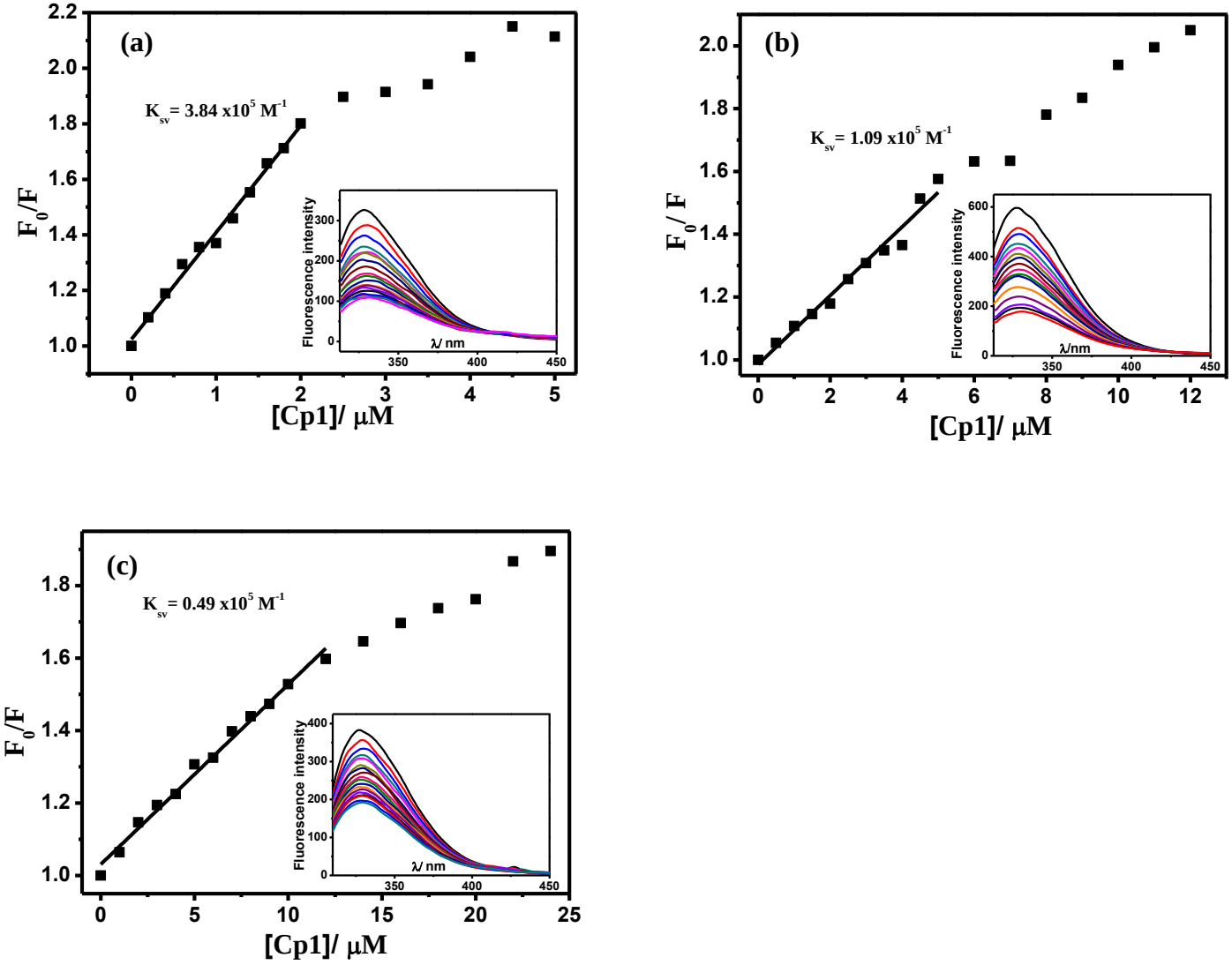

Figure S1. (a), **(b)** and **(c)** represent the fluorescence quenching and Stern-Volmer plots for CprB protein at concentrations 1.50 µM, 3.75 µM and 7.50 µM respectively, with the quencher Cp1.

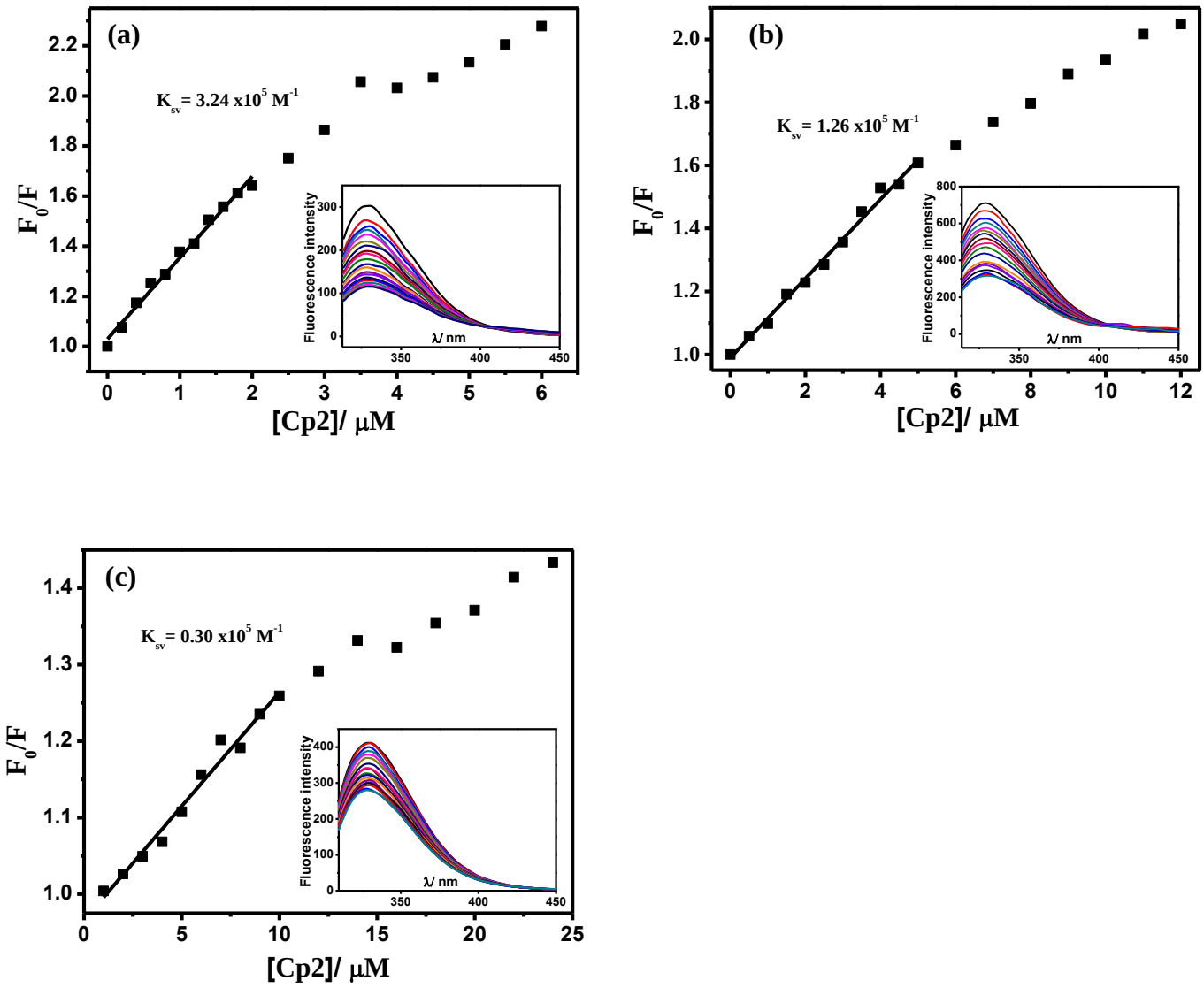

Figure S2. **(a)**, **(b)** and **(c)** represent the fluorescence quenching and Stern-Volmer plots for CprB protein at concentrations 1.50 μM, 3.75 μM and 7.50 μM respectively, with the quencher Cp2.

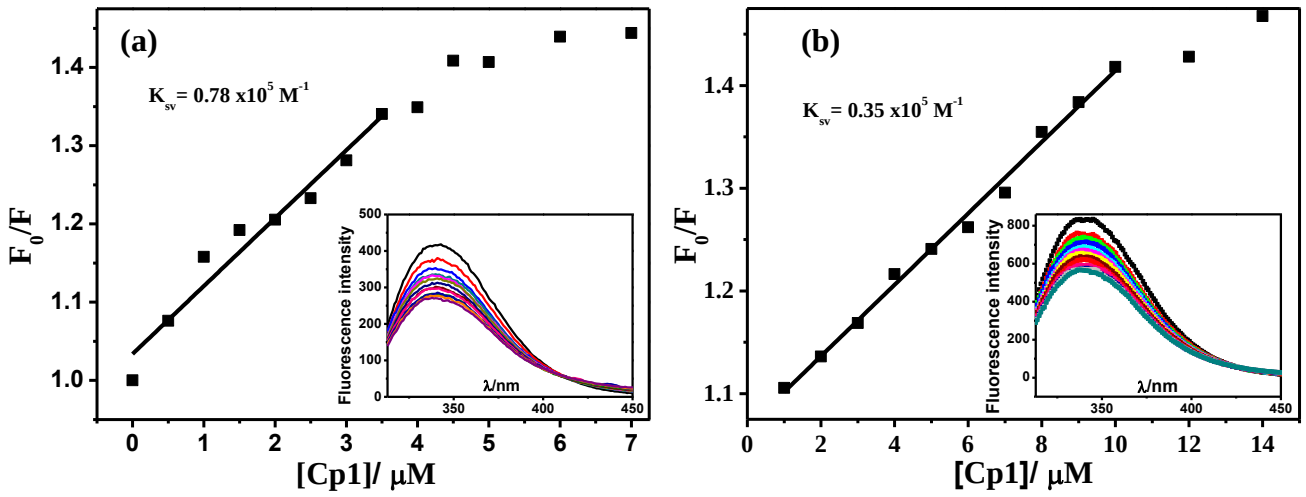

Figure S3. **(a)** and **(b)** represent the fluorescence quenching and Stern-Volmer plots for mutant W185L at concentrations 3.75 μM and 7.50 μM respectively, with the quencher Cp1.

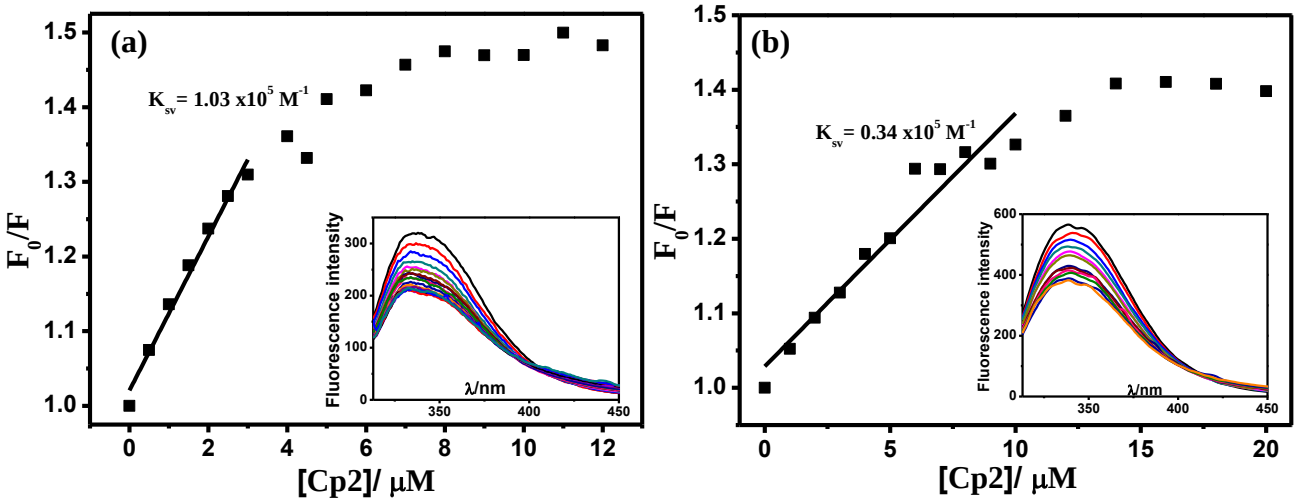

Figure S4. **(a)** and **(b)** represent the fluorescence quenching and Stern-Volmer plots for mutant W185L at concentrations 3.75 μM and 7.50 μM respectively, with the quencher Cp2.

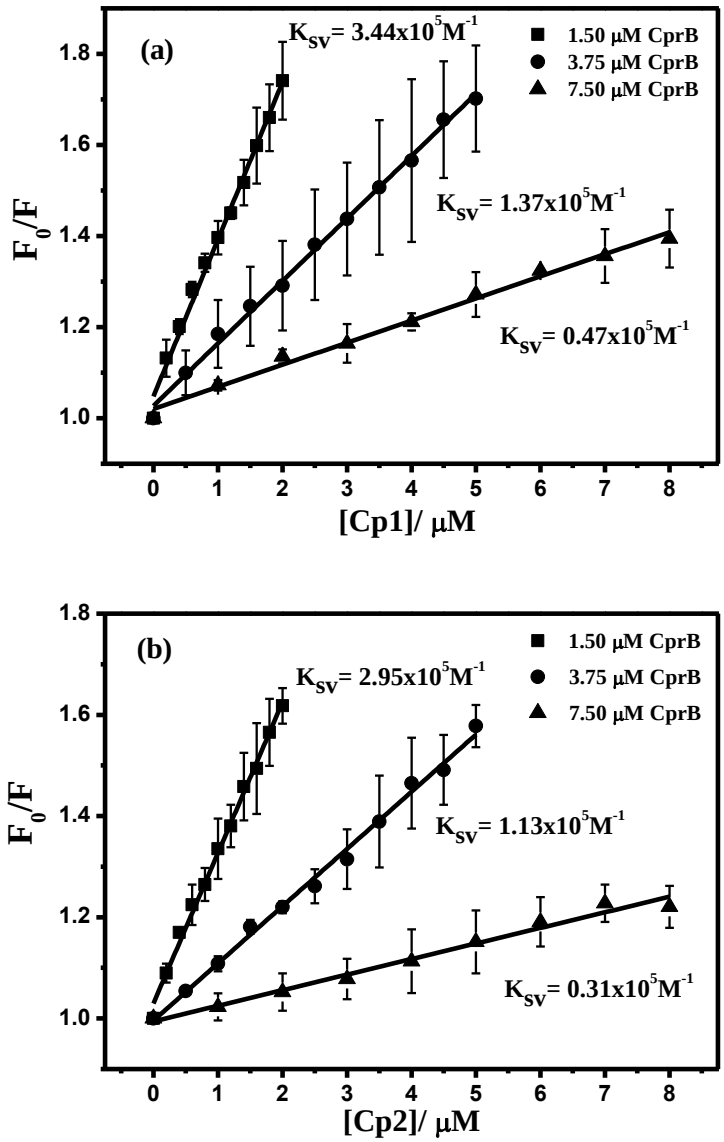

Figure S5. The Stern-Volmer plots for the native CprB at concentrations 1.50 μM, 3.75 μM and 7.50 μM with compounds Cp1 **(a)** and Cp2 **(b)**. (**Figure 7** of main paper with error bars included).

NMR Spectra for compounds Cp1 and Cp2

For all NMR spectra, peaks for grease have been marked as G.

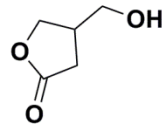

Cp1, ^{1}H NMR

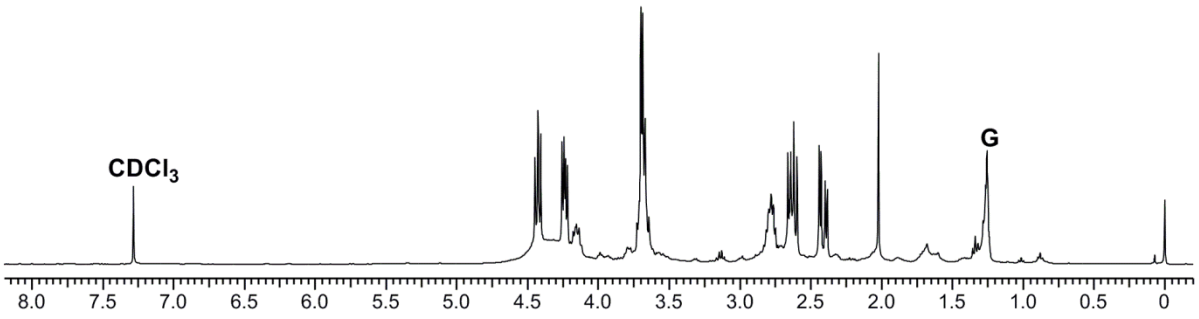

Cp1, ^{13}C NMR

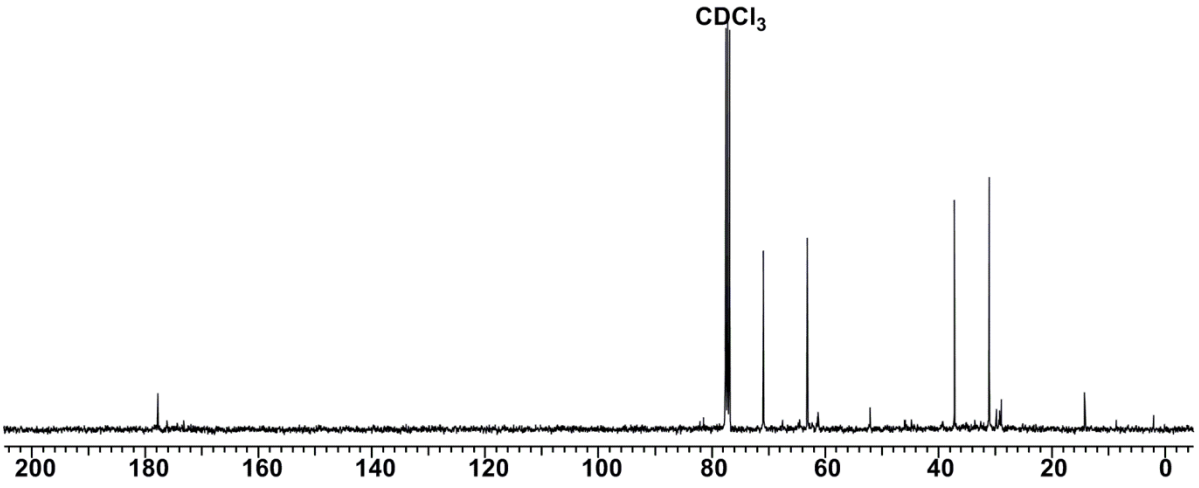

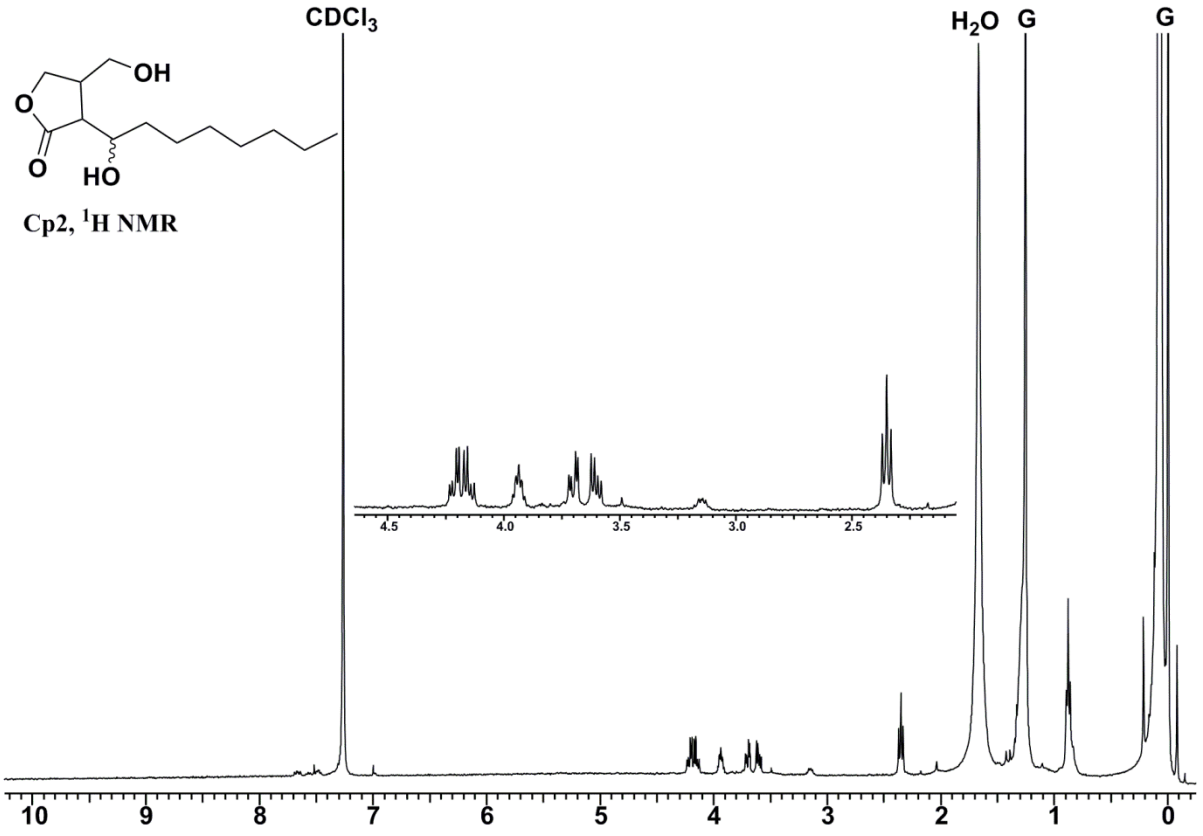

Cp2, ^{1}H NMR

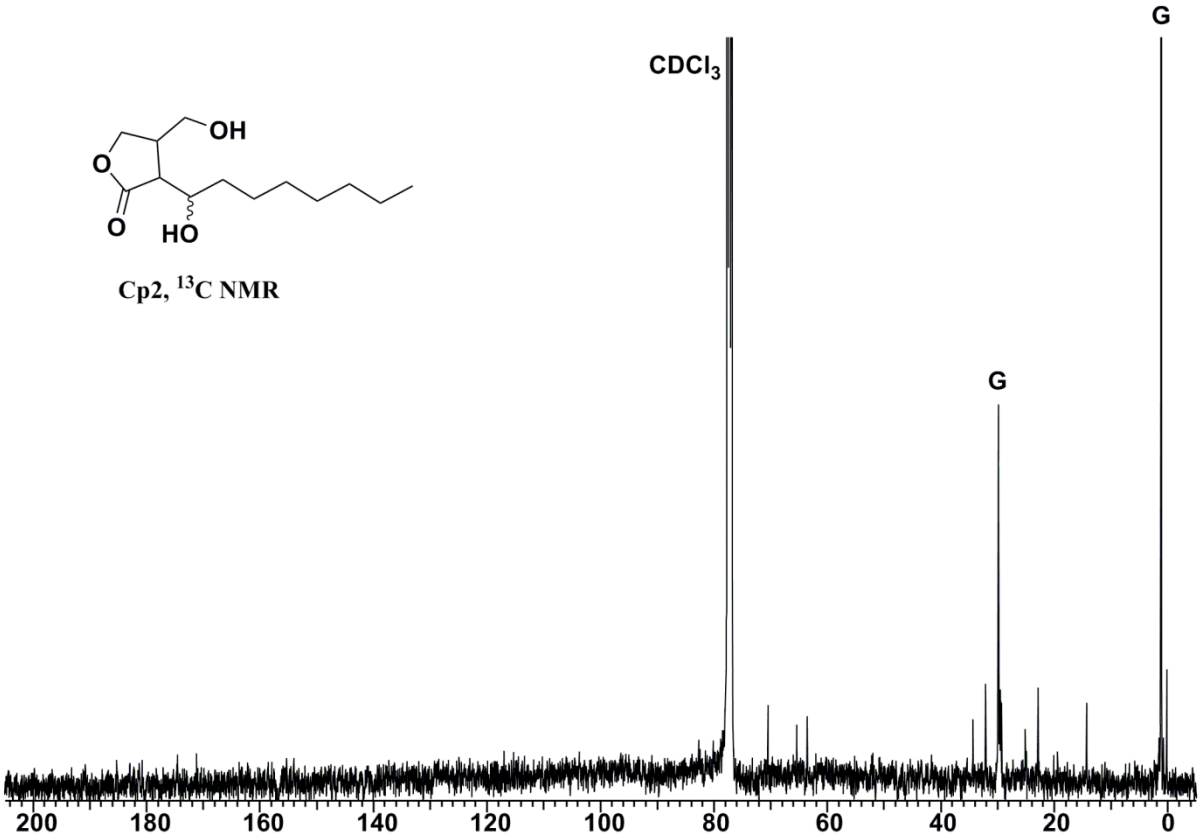

Cp2, ^{13}C NMR

References:

(1) Yamada, Y.; Sugamura, K.; Kondo, K.; Yanagimoto, M.; Okada, H. The Structure of Inducing Factors for Virginiamycin Production in *Streptomyces virginiae*. *J. Antibiot.* **1987**, *40*, 496–504.

(2) Weber, W.; Schoenmakers, R.; Spielmann, M.; El-Baba, M. D.; Folcher, M.; Keller, B.; Weber, C. C.; Link, N.; van de Wetering, P.; Heinzen, C.; Jolivet, B.; Sequin, U.; Aubel, D.; Thompson, C. J.; Fussenegger, M. Streptomyces-derived Quorum-sensing Systems Engineered for Adjustable Transgene Expression in Mammalian Cells and Mice. *Nucleic. Acids Res.* **2003**, *31*, e71.

(3) Takano, E.; Nihira, T.; Hara, Y.; Jones, J. J.; Gershater, C. J.; Yamada, Y.; Bibb, M. Purification and Structural Determination of SCB1, a Gamma-butyrolactone that Elicits Antibiotic Production in Streptomyces coelicolor A3(2). *J. Biol. Chem.* **2000**, *275*, 11010–11016.

References from main paper with more than 10 authors:

(12) Holden, M. T.; Ram, C. S.; de Nys, R.; Stead, P.; Bainton, N. J.; Hill, P. J.; Manefield, M.; Kumar, N.; Labatte, M.; England, D.; Rice, S.; Givskov, M.; Salmond, G. P.; Stewart, G. S.; Bycroft, B. W.; Kjelleberg, S.; Williams, P. Quorum-sensing Cross Talk: Isolation and Chemical Characterization of Cyclic Dipeptides from Pseudomonas aeruginosa and Other Gram-negative Bacteria. *Mol. Microbiol.* **1999**, *33*, 1254–1266.

(27) Weber, W.; Schoenmakers, R.; Spielmann, M.; El-Baba, M. D.; Folcher, M.; Keller, B.; Weber, C. C.; Link, N.; van de Wetering, P.; Heinzen, C.; Jolivet, B.; Sequin, U.; Aubel, D.; Thompson, C. J.; Fussenegger, M. Streptomyces-derived Quorum-sensing Systems Engineered for Adjustable Transgene Expression in Mammalian Cells and Mice. *Nucleic. Acids Res.* **2003**, *31*, e71.